BNL-82116-2009-JA

GEOPHYSICAL RESEARCH LETTERS, VOL. 36, L10801, doi:10.1029/2009GL038216, 2009

Cloud droplet spectral dispersion and the indirect aerosol effect: Comparison of two treatments in a GCM

Leon D. Rotstayn[1] and Yangang Liu[2]

Received 17 March 2009; accepted 10 April 2009; published 19 May 2009.

[1] Two parameterizations of cloud droplet spectral dispersion and their impact on the indirect aerosol effect are compared in a global climate model. The earlier scheme specifies β, the ratio of droplet effective radius to volume-mean radius, in terms of N, the cloud droplet number concentration. The new scheme specifies β in terms of mean droplet mass (L/N), where L is liquid water content, to account for the effect of variations in L. For low to moderate N, the new scheme gives a stronger increase of β with increasing N than the old scheme. In a present-climate simulation, the new scheme shows a stronger gradient between remote regions (small β) and polluted/continental regions (large β). The new scheme also offsets the first indirect aerosol forcing (ΔF) more strongly: $\Delta F = -0.65$ W m^{-2} with constant β, -0.43 W m^{-2} with the old β, and -0.38 W m^{-2} with the new β. **Citation:** Rotstayn, L. D., and Y. Liu (2009), Cloud droplet spectral dispersion and the indirect aerosol effect: Comparison of two treatments in a GCM, *Geophys. Res. Lett.*, *36*, L10801, doi:10.1029/2009GL038216.

1. Introduction

[2] The indirect aerosol effects are the most uncertain components of the anthropogenic radiative forcing of climate. The first indirect effect, whereby aerosols modify cloud-droplet effective radius, was given an uncertainty range of -0.3 to -1.7 W m^{-2} by *Forster et al.* [2007]. The second indirect effect, whereby aerosols modify cloud formation and lifetime, was not strictly considered to be a radiative forcing by *Forster et al.* [2007], but global climate models (GCMs) that include both effects can produce a negative radiative perturbation as large as -2.3 W m^{-2} [*Ming et al.*, 2005]. Such large effects are difficult to reconcile with observed temperature records [*Anderson et al.*, 2003], and this has motivated a search for factors that may cause their magnitude to be overestimated in GCMs.

[3] For example, there is evidence that increases in the width of the cloud droplet spectrum with increasing aerosol loading may reduce the magnitude of the first indirect effect. *Liu and Daum* [2002] compiled observations that showed an increase in the relative dispersion ϵ of the cloud droplet spectrum with increasing cloud droplet number concentration N; ϵ is the ratio of the standard deviation to the mean radius of the cloud droplet number size distribution. The effective radius ratio β, which relates the volume-averaged mean droplet radius r_v to the effective radius r_e ($r_e = \beta r_v$), is an increasing function of ϵ, so β also tends to increase with N. The resultant increase in r_e with increasing aerosol loading was estimated by *Liu and Daum* [2002] to offset the first indirect effect by between 10 and 80%. Tests in GCMs confirmed that including a parameterization of increasing β with N reduced the magnitude of the predicted first indirect effect [*Rotstayn and Liu*, 2003] and total indirect effect [*Peng and Lohmann*, 2003].

[4] Subsequent studies yielded more insight into the underlying mechanism of the dispersion effect. Parcel modeling by *Peng et al.* [2007] showed that an increase of aerosol number concentration at cloud base reduced the supersaturation, which resulted in a slower particle growth rate, so more cloud droplets remained small. This extended the droplet spectra towards smaller sizes and increased the spectral width. Sensitivity studies showed that the dispersion effect decreased for increasing updraft velocity w. Their results were consistent with an analytical expression for ϵ developed by *Liu et al.* [2006], which also indicated a positive correlation between ϵ and N, and a negative correlation between ϵ and w. A parcel-model study by *Yum and Hudson* [2005] also indicated that ϵ should be negatively correlated with w. However, other studies show that there is still no consensus about the mechanism of the dispersion effect [*Lu and Seinfeld*, 2006; *Lu et al.*, 2007].

[5] Earlier parameterizations of the dispersion effect in GCMs specified β solely as a function of N. According to the above discussion, variations in w, which lead to a negative correlation between β and N, may account for some of the scatter in the $\beta - N$ relationship. Another deficiency of representing the dispersion effect in terms of N is its neglect of the effect of variations of liquid water content (L) on ϵ. For example, condensational growth increases L but decreases ϵ [*Rogers and Yau*, 1989]. It is therefore desirable to have a representation of the dispersion effect that includes the effects of variations in L. Further, *Wood* [2000] empirically demonstrated that β is better parameterized in terms of r_v than N. These arguments motivated *Liu et al.* [2008a] to analyze data from several field projects, to fit a parameterization of β in terms of mean droplet mass (L/N). They analytically estimated that the dispersion effect would reduce the first indirect effect by 42%.

[6] In this letter, we compare the new parameterization of β from *Liu et al.* [2008a] with one of the earlier N-dependent parameterizations in a GCM. In Section 2, the two parameterizations of β and the GCM simulations are

[1]Centre for Australian Weather and Climate Research, CSIRO Marine and Atmospheric Research, Aspendale, Victoria, Australia.

[2]Atmospheric Sciences Division, Brookhaven National Laboratory, Upton, New York, USA.

0094-8276/09/2009GL038216$05.00

described. Section 3 contains results and discussion, and Section 4 contains a summary.

2. Parameterizations and GCM Simulations

[7] *Liu et al.* [2008a] empirically derived

$$\beta = 0.07\left(\frac{L}{N}\right)^{-0.14}, \quad (1)$$

where L is in g cm^{-3} and N is in cm^{-3} (CGS units) [see *Liu et al.*, 2008a, Figure 4]. We compare equation (1) ("NEWBETA") with the N-dependent parameterization ("OLDBETA") used by *Rotstayn and Liu* [2003], namely

$$\beta = \frac{(1+2\epsilon^2)^{2/3}}{(1+\epsilon^2)^{1/3}}, \quad (2)$$

where

$$\epsilon = 1 - 0.7\exp(-0.003N), \quad (3)$$

which is shown as the middle curve in Figure 1 of *Rotstayn and Liu* [2003]. We also perform simulations with a fixed value of β, as commonly used in GCMs for many years. *Pontikis and Hicks* [1992] proposed $\beta = 1.1$, a value that is still used in some recent GCMs [e.g., *Quaas et al.*, 2004]. A widely used specification is based on measurements in stratocumulus by *Martin et al.* [1994], namely $\beta = 1.08$ over oceans and $\beta = 1.14$ over land, which gives a global-mean value close to 1.1. For simplicity, we use $\beta = 1.1$, and refer to this scheme as "FIXBETA".

[8] We use a low-resolution version of the CSIRO GCM, described by *Rotstayn et al.* [2007]. The model has an interactive aerosol scheme, which treats the sulfur cycle, carbonaceous aerosol, dust and sea salt; see *Rotstayn et al.* [2007] for a detailed evaluation. The only material change from *Rotstayn et al.* [2007] concerns the parameterization of N, which is now based on the empirical scheme used by *Quaas et al.* [2004]:

$$N = 162 m_a^{0.41}, \quad (4)$$

where m_a is the aerosol mass concentration in μg m^{-3}. As done by *Quaas et al.* [2004], we take m_a as the maximum of the masses of the submicron hydrophilic aerosol species in the GCM (sulfate, submicron sea salt, and hydrophilic carbonaceous aerosol); carbonaceous aerosol is the sum of organic matter and black carbon. *Rotstayn et al.* [2007] parameterized N following *Menon et al.* [2002] in their coupled ocean-atmosphere simulations of 20th Century climate change, but found it necessary to "tune" that parameterization to obtain a net aerosol forcing substantially smaller in magnitude than the anthropogenic greenhouse gas forcing. The motivation for changing to a different parameterization of N was to avoid the need to tune the parameters. We note that such empirical curve fits cannot capture the complexity of aerosol-cloud interactions, and that there has been much progress in the development of mechanistic parameterizations of cloud-droplet nucleation [e.g., *Fountoukis and Nenes*, 2005].

[9] All simulations use climatological sea-surface temperatures and sea ice, and levels of greenhouse gases for the year 2000. Emissions of aerosols and aerosol precursors are specified for either 2000 ("PD" runs) or 1870 ("PI" runs), using the inventories described by *Rotstayn et al.* [2007]. We performed three pairs of (PD and PI) runs to estimate the first indirect effect. In these runs, the aerosol direct effect was turned off, and equation (4) was used to specify N in the radiation scheme but a fixed N = 100 cm^{-3} was used in the autoconversion scheme to suppress the second indirect effect. Also, to suppress changes in the meteorology between the PD and PI runs in each pair, two calls were made to the shortwave (SW) radiation scheme at each time step. The first call used N from equation (4), while the second call used N = 100 cm^{-3} to calculate the effect of SW radiation on the meteorology. Diagnostics from the first call were saved to enable calculation of β, r_e and the change in the SW flux ΔF at the top of the atmosphere (TOA) due to the difference in N between the two calls. ΔF is not physically meaningful in itself, but $\Delta F_{\mathrm{PD}} - \Delta F_{\mathrm{PI}}$ provides a measure of the first indirect effect as a "pure" forcing, which is unaffected by feedbacks or changes in meteorology (A. Jones, personal communication, 2008). We neglect the longwave (LW) component of the first indirect forcing, because it is less than 0.01 W m^{-2} in the global mean in our model. These pairs of runs are respectively denoted NEWBETA, OLDBETA and FIXBETA, depending on the specification of β as described above. These runs were integrated for 10 years after a three-month spinup. Uncertainty ranges are 95% confidence intervals, based on a t-test using the annual means as independent data points.

3. Results and Discussion

[10] First, we note that the modeled global-mean cloud fields in the NEWBETA-PD run have no large biases that are likely to adversely affect our results. Global-mean cloud cover (67%), liquid-water path over oceans (69 g m^{-2}), SW cloud forcing (-51 W m^{-2}), LW cloud forcing (31 W m^{-2}), and r_e (10.5 μm) are in reasonable agreement with observations [cf. *Rotstayn*, 1998; *Rotstayn and Liu*, 2003].

[11] To illustrate the difference between the two schemes and the effect of variations of L on β, Figure 1 shows plots of β versus N using OLDBETA (equation (2)), and NEWBETA (equation (1)) for L = 0.03, 0.1 and 0.3 g m^{-2} (taken to represent low, mid-range and high values of L); note change of units from equation (1). Also shown is a scatter plot of points saved from one day of the NEWBETA-PD run. The scatter plot confirms that the chosen values of L are representative of low, mid-range and high values. The curves show that in the low to middle range of N (up to about 150 cm^{-3}), the gradient ($\Delta\beta/\Delta N$) is larger using NEWBETA, especially for low values of L. Note also that NEWBETA allows points to occur with $\beta < 1$. Such observations are probably associated with negatively skewed droplet spectra [*Liu et al.*, 2008b].

[12] Figure 2 shows the simulated distribution of β for the present climate using both schemes. To obtain the column-averaged value of β at each time step, the value in each layer was weighted by its liquid-water path. The NEWBETA scheme gives a stronger gradient of β between remote regions (small β) and polluted/continental regions

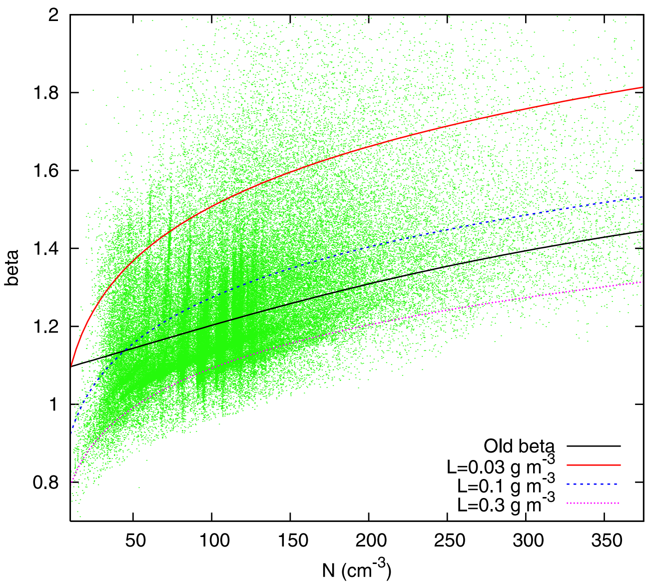

Figure 1. Plot of β versus N using OLDBETA (equation (2)) – black curve) and NEWBETA (equation (1)) for low, mid-range and high values of L (colored curves). Also shown as green dots are points saved from one day of the NEWBETA-PD run (1 July in the final year).

(large β) than the OLDBETA scheme, consistent with Figure 1. The difference between NEWBETA and OLDBETA is especially noticeable over central Asia, where low L (not shown) enhances $\Delta\beta/\Delta N$ in NEWBETA (Figure 1). However, the global-mean values are essentially identical for the two schemes, being 1.23 in both cases. This is somewhat larger than the values that have often been prescribed in GCMs ($\beta \approx 1.1$).

[13] The differences in β between PD and PI runs are shown in Figure 3 for the two schemes. In both cases, changes in β are due to changes in N (since L is forced to be identical in the PD and PI runs of each pair). NEWBETA gives larger changes in β over polluted regions than OLDBETA, confirming that, for fixed L, the dependence of β on N tends to be stronger in NEWBETA than in OLDBETA. The increase in global-mean β is larger in NEWBETA (0.031) than in OLDBETA (0.023). Accordingly, the decrease in global-mean r_e is smaller in NEWBETA (-0.36 μm) than in OLDBETA (-0.42 μm), compared to -0.55 μm in FIXBETA.

[14] The above discussion suggests that NEWBETA should more strongly offset the global-mean first indirect effect than OLDBETA. This is indeed the case; see Table 1. Compared to FIXBETA ($\Delta F = -0.65 \pm 0.006$ W m^{-2}), the reduction in the first indirect effect is 34% in OLDBETA (-0.43 ± 0.005 W m^{-2}) and 42% in NEWBETA (-0.38 ± 0.003 W m^{-2}). The reduction of 42% in NEWBETA is very similar to the analytical estimate from *Liu et al.* [2008a], though this result may be model-dependent. Note that the difference between OLDBETA and NEWBETA is not large in the global mean. This is reassuring, in the sense that two parameterizations of β derived by different approaches give results that are of similar magnitude. However, Table 1 shows that the difference in forcing between NEWBETA

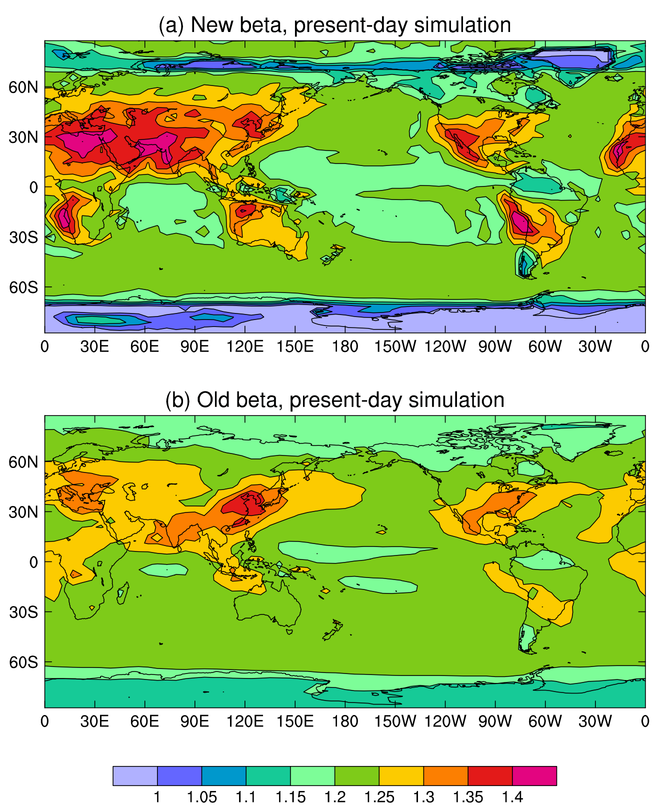

Figure 2. Simulated distribution of the effective radius ratio β using (a) equation (1) (NEWBETA-PD run), and (b) equation (2) (OLDBETA-PD run).

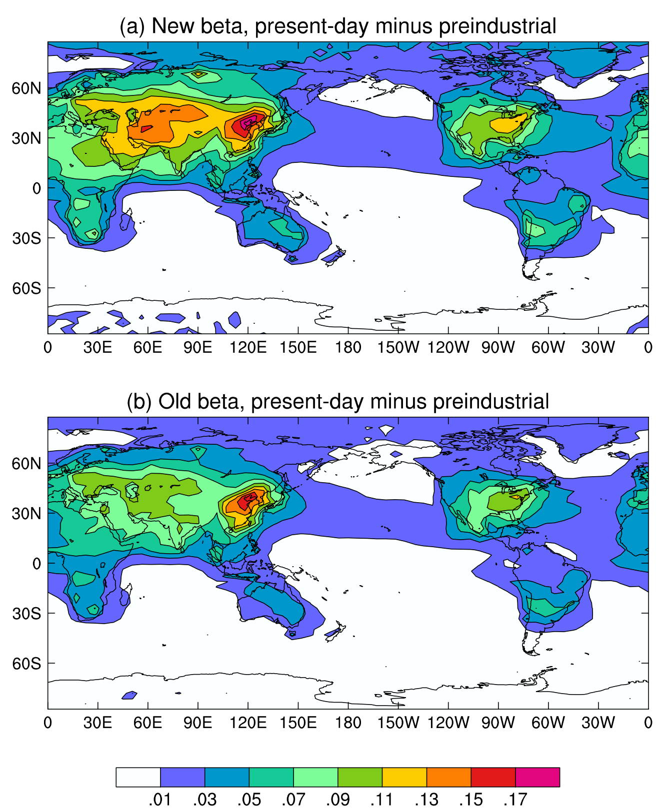

Figure 3. Difference of the effective radius ratio β between (a) the NEWBETA-PD and NEWBETA-PI runs, and (b) the OLDBETA-PD and OLDBETA-PI runs.

Table 1. SW First Indirect Aerosol Forcing Obtained With the FIXBETA, OLDBETA and NEWBETA Treatments (W m^{-2})

	FIXBETA	OLDBETA	NEWBETA
Global	−0.65	−0.43	−0.38
Land	−0.98	−0.69	−0.57
Ocean	−0.51	−0.33	−0.30

and OLDBETA is larger over land than over oceans, both in absolute and relative terms; this is consistent with the larger (PD minus PI) changes in β over land in NEWBETA than in OLDBETA (Figure 3).

[15] Does the new β still give a larger reduction in the indirect aerosol effect if the second indirect effect is activated in the GCM? This question arises because an increase of L in the PD runs relative to the PI runs would reduce β in equation (1). We therefore performed a further three pairs of PD and PI runs, in which the aerosol-dependent N was allowed to affect autoconversion as well as droplet effective radius; these pairs of runs are denoted NEWBETA12, OLDBETA12 and FIXBETA12. As in the earlier runs, direct aerosol effects were suppressed, so the total (first and second) indirect effect can be estimated from the change in SW flux at the TOA between the PD and PI runs of each pair. Each run was integrated for 50 years after a three-month spinup, to allow for the larger variability in these runs, in which the meteorology differs between the PD and PI runs of each pair.

[16] Interestingly, the total indirect effect is still offset a little more strongly in NEWBETA12 than in OLDBETA12. We obtained SW flux perturbations at the TOA of -1.03 ± 0.03 W m^{-2}, -0.72 ± 0.04 W m^{-2} and -0.62 ± 0.03 W m^{-2} in FIXBETA12, OLDBETA12 and NEWBETA12 respectively. As expected, NEWBETA12-PD does show a small increase of global-mean liquid-water path relative to NEWBETA12-PI (from 64.4 to 65.0 g m^{-2}, or about 1%). The change in liquid-water cloud fraction from NEWBETA12-PI to NEWBETA12-PD is negligible (39.93% to 39.97%), so the relative change in liquid-water path can be used as a proxy for the relative change in L. The effect of increased L is roughly balanced by a larger change in global-mean N ($\Delta N = N_{PD} - N_{PI}$) in the runs that include the second indirect effect, due to reduced wet scavenging of aerosol in the PD runs relative to the PI runs. (Column-averaged values of N at each time step were obtained by weighting N in each layer by its liquid-water path.) For example, ΔN = 24.3 cm^{-3} in NEWBETA12, compared to 22.7 cm^{-3} in NEWBETA. To put this in context, N = 108.4 cm^{-3} in NEWBETA-PI and N = 109.5 cm^{-3} in NEWBETA12-PI, so $\Delta N/N$ = 20.9% in NEWBETA and 22.2% in NEWBETA12. This means that $\Delta(L/N) = (L/N)_{PD} - (L/N)_{PI}$ is about −17.3% in NEWBETA (in which L is fixed) and −17.4% in NEWBETA12. Thus the scavenging feedback on N explains why the difference in SW flux perturbation between OLDBETA12 and NEWBETA12 is similar to the difference in the first indirect effect between OLDBETA and NEWBETA. It also explains why changing from FIXBETA to OLDBETA gives a larger reduction in the magnitude of indirect effects (~0.3 W m^{-2}) when both effects are considered than when only the first effect is considered (~0.2 W m^{-2}).

4. Summary

[17] We compared two parameterizations of β and their impact on the indirect aerosol effect in the CSIRO GCM. The first scheme specifies β solely in terms of N [*Liu and Daum*, 2002; *Rotstayn and Liu*, 2003]. This scheme was compared to a new approach [*Liu et al.*, 2008a], which accounts for the effect of variations in L: $\beta \sim (L/N)^{-0.14}$. A plot of β versus N showed that for low to moderate N, the new scheme gives a stronger increase of β with increasing N than the old scheme, especially for small L. In a present-climate simulation, the new scheme showed a stronger gradient between remote regions (small β) and polluted/continental regions (large β), but both schemes gave global-mean β = 1.23. This is somewhat larger than values often prescribed in GCMs ($\beta \approx 1.1$). The difference of present-day (PD) and preindustrial (PI) runs showed a larger increase of β with the new scheme, and a smaller decrease of effective radius.

[18] Consistent with the above, the new scheme offset the first indirect aerosol forcing (ΔF) more strongly than the old scheme. In the global mean, $\Delta F = -0.65$ W m^{-2} with β = 1.1, −0.43 W m^{-2} with the N-dependent β, and −0.38 W m^{-2} with the new β. The reduction of 42% with the new β is very similar to the analytical estimate from *Liu et al.* [2008a], though this is may be model-dependent. For the combined (first and second) indirect effects, we obtained SW radiative perturbations of −1.03 W m^{-2} with β = 1.1, −0.72 W m^{-2} with the N-dependent β and −0.62 W m^{-2} with the new β. In other words, a stronger offset due to the new β was also obtained when the second indirect effect was enabled in the GCM. This was due to compensating effects of changes in L and N on the function $(L/N)^{-0.14}$: Although the difference of PD and PI runs showed a modest increase of liquid-water path, there was also a larger increase of N than in the runs that only included the first indirect effect. The larger change of N in the runs that included the second indirect effect was due to reduced wet scavenging of aerosol in the PD runs relative to the PI runs – a good example of the subtle feedbacks that can occur in the aerosol-cloud-climate problem. Important extensions that we have not considered include the sensitivity of our results to the method of parameterizing N, and to the baseline state of the clouds in the model.

[19] **Acknowledgments.** LR was supported in part by the Australian Climate Change Science Program (ACCSP). YL was supported by the ARM and ASP programs of the US Department of Energy (DOE).

References

Anderson, T. L., R. J. Charlson, S. E. Schwartz, R. Knutti, O. Boucher, H. Rodhe, and J. Heintzenberg (2003), Climate forcing by aerosols—A hazy picture, *Science*, *300*, 1103–1104.

Forster, P., et al. (2007), Changes in atmospheric constituents and in radiative forcing, in *Climate Change 2007: The Physical Science Basis. Contribution of Working Group I to the Fourth Assessment Report of the Intergovernmental Panel on Climate Change*, edited by S. Solomon et al., pp. 129–234, Cambridge Univ. Press, Cambridge, U. K.

Fountoukis, C., and A. Nenes (2005), Continued development of a cloud droplet formation parameterization for global climate models, *J. Geophys. Res.*, *110*, D11212, doi:10.1029/2004JD005591.

Liu, Y., and P. H. Daum (2002), Indirect warming effect from dispersion forcing, *Nature*, *419*, 580–581.

Liu, Y., P. H. Daum, and S. S. Yum (2006), Analytical expression for the relative dispersion of the cloud droplet size distribution, *Geophys. Res. Lett.*, *33*, L02810, doi:10.1029/2005GL024052.

Liu, Y., P. H. Daum, H. Guo, and Y. Peng (2008a), Dispersion bias, dispersion effect and aerosol-cloud conundrum, *Environ. Res. Lett.*, *3*, 045021, doi:10.1088/1748-9326/3/4/045021.

Liu, Y., P. H. Daum, and S. S. Yum (2008b), Ship tracks revisited: New understanding and cloud parameterization, *Asia Pac. J. Atmos. Sci.*, *44*, 1–9.

Lu, M.-L., and J. H. Seinfeld (2006), Effect of aerosol number concentration on cloud droplet dispersion: A large-eddy simulation study and implications for aerosol indirect forcing, *J. Geophys. Res.*, *111*, D02207, doi:10.1029/2005JD006419.

Lu, M.-L., W. C. Conant, H. H. Jonsson, V. Varutbangkul, R. C. Flagan, and J. H. Seinfeld (2007), The Marine Stratus/Stratocumulus Experiment (MASE): Aerosol-cloud relationships in marine stratocumulus, *J. Geophys. Res.*, *112*, D10209, doi:10.1029/2006JD007985.

Martin, G. M., D. W. Johnson, and A. Spice (1994), The measurement and parameterization of effective radius of droplets in warm stratocumulus clouds, *J. Atmos. Sci.*, *51*, 1823–1842.

Menon, S., A. D. Del Genio, D. Koch, and G. Tselioudis (2002), GCM simulations of the aerosol indirect effect: Sensitivity to cloud parameterization and aerosol burden, *J. Atmos. Sci.*, *59*, 692–713.

Ming, Y., V. Ramaswamy, P. A. Ginoux, L. W. Horowitz, and L. M. Russell (2005), Geophysical Fluid Dynamics Laboratory general circulation model investigation of the indirect radiative effects of anthropogenic sulfate aerosol, *J. Geophys. Res.*, *110*, D22206, doi:10.1029/2005JD006161.

Peng, Y., and U. Lohmann (2003), Sensitivity study of the spectral dispersion of the cloud droplet size distribution on the indirect aerosol effect, *Geophys. Res. Lett.*, *30*(10), 1507, doi:10.1029/2003GL017192.

Peng, Y., U. Lohmann, R. Leaitch, and M. Kulmala (2007), An investigation into the aerosol dispersion effect through the activation process in marine stratus clouds, *J. Geophys. Res.*, *112*, D11117, doi:10.1029/2006JD007401.

Pontikis, C., and E. Hicks (1992), Contribution to the cloud droplet effective radius parameterization, *Geophys. Res. Lett.*, *19*, 2227–2230, doi:10.1029/92GL02283.

Quaas, J., O. Boucher, and F.-M. Bréon (2004), Aerosol indirect effects in POLDER satellite data and the Laboratoire de Météorologie Dynamique-Zoom (LMDZ) general circulation model, *J. Geophys. Res.*, *109*, D08205, doi:10.1029/2003JD004317.

Rogers, R. R., and M. K. Yau (1989), *A Short Course in Cloud Physics*, 3rd ed., 293 pp., Pergamon, Oxford, U. K.

Rotstayn, L. D. (1998), A physically based scheme for the treatment of stratiform clouds and precipitation in large-scale models. II: Comparison of modelled and observed climatological fields, *Q. J. R. Meteorol. Soc.*, *124*, 389–415.

Rotstayn, L. D., and Y. Liu (2003), Sensitivity of the first indirect aerosol effect to an increase of cloud droplet spectral dispersion with droplet number concentration, *J. Clim.*, *16*, 3476–3481.

Rotstayn, L. D., et al. (2007), Have Australian rainfall and cloudiness increased due to the remote effects of Asian anthropogenic aerosols?, *J. Geophys. Res.*, *112*, D09202, doi:10.1029/2006JD007712.

Wood, R. (2000), Parametrization of the effect of drizzle upon the droplet effective radius in stratocumulus clouds, *Q. J. R. Meteorol. Soc.*, *126*, 3309–3324.

Yum, S. S., and J. G. Hudson (2005), Adiabatic predictions and observations of cloud droplet spectral broadness, *Atmos. Res.*, *73*, 203–223.

Y. Liu, Atmospheric Sciences Division, Brookhaven National Laboratory, Building 815E, 75 Rutherford Drive, Upton, NY 11973, USA. (lyg@bnl.gov)

L. D. Rotstayn, Centre for Australian Weather and Climate Research, CSIRO Marine and Atmospheric Research, Private Bag 1, Aspendale, Vic 3195, Australia. (leon.rotstayn@csiro.au)